Aerodynamic Aspects of Aircraft Dynamics at High Angles of Attack

K. J. Orlik-Rückemann
National Research Council of Canada, Ottawa, Ontario, Canada

Introduction

TO achieve tactical superiority in the air, a fighter aircraft must be capable of high-performance maneuvers. To perform such maneuvers, the aircraft must be able to carry out controlled flight at high angles of attack. To safely predict and analyze such flight conditions, our understanding of the aerodynamics of aircraft at high angles of attack (high α) may require further improvements.

In the context of this review, the aerodynamic phenomena at high α will be discussed mainly from the point of view of their impact on stability parameters of an aircraft. Adequate knowledge of these parameters is required for the prediction of an aircraft's behavior before departure, for the description of its departure/spin-resistance characteristics, and for the difficult analysis of the flight range between the departure and the fully developed spin, if such an analysis is required. Stability parameters are needed also for the assessment of the tracking capabilities of an aircraft, for the efficient design of the control system, and for the evaluation of the range of maneuvers that can safely be induced by the pilot. Such maneuvers at high angles of attack are not only relevant in situations involving air combat and missile avoidance actions, but may also be necessary during certain phases of the landing approach.

Flow Phenomena in Steady and Oscillatory Flight at High Angles of Attack

The aerodynamics of an aircraft performing a *steady* flight at high angles of attack has been studied for several years and a considerable amount of information is now available in this area.[1,2] It is well known that such an aircraft is exposed to a variety of flow phenomena that usually are nonexistent or have much less significance at lower angles of attack. These phenomena encompass all kinds of transitional, separated, and vortical flows over the body, the wings, and the control surfaces of the aircraft. Of particular interest herein are those flow phenomena that significantly vary with the angle of attack and that, at high enough values of that parameter, can cause asymmetric effects even if the aircraft itself continues to head symmetrically into the wind (i.e., has zero sideslip). Two of the most important phenomena of that kind are 1) the formation and asymmetric shedding of forebody vortices and 2) the formation and asymmetric bursting of wing leading-edge vortices. It is also known that the behavior of the forebody vortices can be affected by blowing[3,4] or by introduction of a mechanical disturbance near the nose of the forebody.

If an *oscillatory* motion is superimposed on the primary steady flight of the aircraft, the aforementioned phenomena become much more involved due to the introduction into an already complex picture of an additional variable, namely, the element of time. Let us consider, for instance, an oscillation in pitch. During such an oscillation the forebody vortices will change their lateral and vertical positions as functions of the angle of attack, which itself is a function of time. Similarly, leading-edge vortices will periodically vary the longitudinal location at which they burst. The various components of the aircraft, such as the fin(s) and the horizontal stabilizer, will move in and out of the local flow regions in which they are embedded. To make matters even more complex, all of these motions will take place not in a manner simultaneous with the motion of the aircraft, but with a certain delay, mainly due to the convective time lag. This delay is a function of the distance of the station under consideration (say, at the fin) from the station at which a particular flow phenomenon originates (in the case of the forebody vortices, at the vicinity of the nose).

The response of the forebody vortices to the oscillatory pitching motion of a symmetrically mounted cone-wing configuration was investigated at the National Aeronautical Establishment (NAE) by flow visualization motion pictures made in a water tunnel. The periodic lateral motion of the vortices as well as the time delay between the motion of the vortices and that of the model could be clearly seen. It is obvious that such a lateral motion of the vortices must cause lateral aerodynamic reactions in response to the pitching motion and that the observed time delay requires a vectorial

---

Dr. Kazimierz J. Orlik-Rückemann, a Principal Research Officer at the National Research Council of Canada, was born in Warsaw, Poland, and obtained his M.Sc., Tekn. Lic. and Tekn. D. degrees in Aeronautical Engineering at the Royal Institute of Technology (K.T.H.) in Stockholm, Sweden. In 1955, after being associated for some years with various aspects of aerodynamic research at the Division of Aeronautics at the K.T.H. and the Aeronautical Research Institute of Sweden (F.F.A.), he moved to the National Aeronautical Establishment (NAE) of the National Research Council in Ottawa, Canada, where he was appointed Head of the High Speed Aerodynamics Laboratory in 1958. In 1963 he became the Head of the newly formed Unsteady Aerodynamics Laboratory which was set up for work on unsteady flow phenomena and dynamic stability problems at high speeds. In 1963-64 he served as Chairman of the Supersonic Tunnel Association, and since 1974 he has been a member of the AGARD Fluid Dynamics Panel where he also served as Chairman in 1980 and 1981. He was for many years an Associate Editor of the *CASI Transactions*. He is a Fellow of the CASI and a Fellow of the AIAA. His present interests encompass high-angle-of-attack aerodynamics, flight mechanics, dynamic experiments in wind tunnels, and problems related to space transportation systems.

Presented as Paper 82-1363 at the AIAA 9th Atmospheric Flight Mechanics Conference, San Diego, Calif., Aug. 9-11, 1982; submitted Sept. 1, 1982; revision received Feb. 18, 1983.

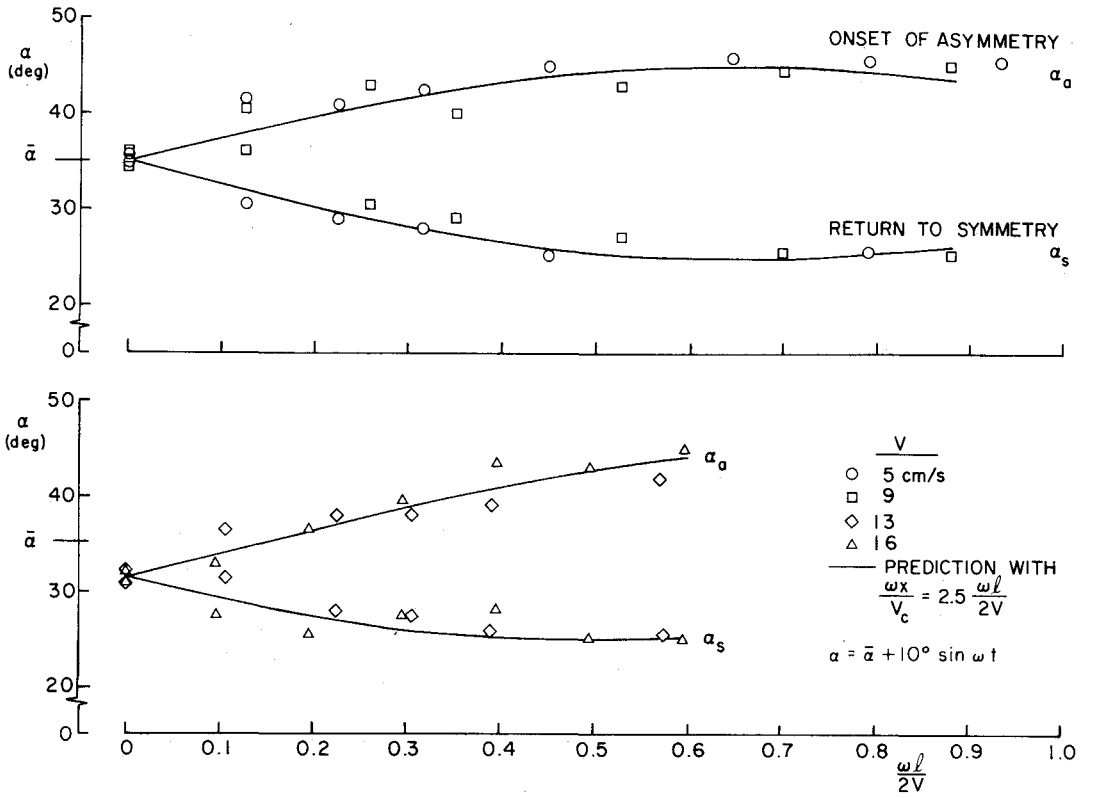

Fig. 1 Phase lag on model oscillating in pitch in water tunnel (NAE).

Table 1 Dynamic moment derivatives

Pure rotation			Translational acceleration			Oscillation around fixed axis		
						Damping derivatives	Cross derivatives	Cross-coupling derivatives
$C_{lp} = \frac{\partial C_l}{\partial \frac{pb}{2V}}$	$C_{mp} = \frac{\partial C_m}{\partial \frac{pb}{2V}}$	$C_{np} = \frac{\partial C_n}{\partial \frac{pb}{2V}}$	$C_{l\dot{\alpha}} = \frac{\partial C_l}{\partial \frac{\dot{\alpha}\bar{c}}{2V}}$	$C_{m\dot{\alpha}} = \frac{\partial C_m}{\partial \frac{\dot{\alpha}\bar{c}}{2V}}$	$C_{n\dot{\alpha}} = \frac{\partial C_n}{\partial \frac{\dot{\alpha}\bar{c}}{2V}}$	$C_{lp} + C_{l\dot{\beta}} \sin\alpha$	$C_{lr} - C_{l\dot{\beta}} \cos\alpha$	$C_{lq} + C_{l\dot{\alpha}}$
						$C_{mq} + C_{m\dot{\alpha}}$	$C_{np} + C_{n\dot{\beta}} \sin\alpha$	$C_{mr} - C_{m\dot{\beta}} \cos\alpha$
$C_{lq} = \frac{\partial C_l}{\partial \frac{q\bar{c}}{2V}}$	$C_{mq} = \frac{\partial C_m}{\partial \frac{q\bar{c}}{2V}}$	$C_{nq} = \frac{\partial C_n}{\partial \frac{q\bar{c}}{2V}}$	$C_{l\dot{\beta}} = \frac{\partial C_l}{\partial \frac{\dot{\beta}b}{2V}}$	$C_{m\dot{\beta}} = \frac{\partial C_m}{\partial \frac{\dot{\beta}b}{2V}}$	$C_{n\dot{\beta}} = \frac{\partial C_n}{\partial \frac{\dot{\beta}b}{2V}}$	$C_{nr} - C_{n\dot{\beta}} \cos\alpha$		$C_{mp} + C_{m\dot{\beta}} \sin\alpha$
								$C_{nq} + C_{n\dot{\alpha}}$
$C_{lr} = \frac{\partial C_l}{\partial \frac{rb}{2V}}$	$C_{mr} = \frac{\partial C_m}{\partial \frac{rb}{2V}}$	$C_{nr} = \frac{\partial C_n}{\partial \frac{rb}{2V}}$						

representation of those reactions, i.e., one in which both the components in phase with the motion of the model and the components in quadrature with that motion (or in phase with the angular rate) have to be considered. When presented in the derivative form, such components are usually referred to as static and dynamic derivatives, respectively, of the aerodynamic reactions with respect to pitching. By repeating the flow visualization motion pictures for several values of water speed V, and oscillation frequency ω, it was possible to obtain the diagram in Fig. 1, showing the angle of attack for the onset of asymmetry, α_a, when α was increasing, and the angle of attack for the return to symmetrical flow conditions, α_s, when α was decreasing during the oscillation. Simple expressions were derived for α_a and α_s in which the phase lag was proportional to the reduced frequency of oscillation, and it is shown here that it was possible to obtain a good correlation between these expressions and the experimental points when the phase lag was assumed to be

$$\omega x/V_c = 2.5(\omega l/2V)$$

where V_c is the convective velocity and x/l is the dimensionless longitudinal coordinate.

The NAE film also demonstrated how the direction of the vortex asymmetry on a symmetrically mounted model could be controlled by normal blowing or by introducing a mechanical disturbance on the forebody.

Another movie film, made in the Northrop water tunnel, showed the relation between the oscillation in roll of a highly swept delta wing and the differential oscillatory displacement of the longitudinal location on the wing at which the vortices emanating from the wing leading edge break down. It is known that vortex-burst location is sensitive to both the angle of attack and the angle of sideslip, and the effective values of these angles on each half of the wing vary periodically as the wing oscillates in roll. Although the time scale of the Northrop experiment was such that phase lags could not easily be observed, it is a safe assumption that such lags must have been present during the experiment, with the resulting static and dynamic aerodynamic reactions due to oscillation in roll.

It should be noted that the oscillatory flow phenomena, that involve shedding of the forebody vortices and their asymmetrical motion, will occur on all oscillating, pointed, slender bodies that fly at a high angle of attack and, therefore, have impact on the dynamics of not only high-performance aircraft but also of missiles. Although this paper deals mostly with problems related to aircraft, much of the material can also be applied to missiles and, indeed, one or two examples of such applications will be included.

Effects on Dynamic Stability Parameters

The aforementioned high-α flow phenomena have large effects on all of the aerodynamic characteristics of the aircraft including, of course, the static and dynamic stability parameters. For the dynamic stability considerations that are the subject of this review, the most important such effects are: 1) large nonlinear variations of stability parameters with angle of attack, angle of sideslip, and rate of coning, as well as with amplitude and frequency of oscillation; 2) significant aerodynamic cross-coupling between longitudinal and lateral degrees of freedom; 3) time-dependent and hysteresis effects; and 4) strong configuration dependence.

Before discussing these effects in some detail, let us first briefly consider the various categories of dynamic stability derivatives. For simplicity, the discussion will be restricted to dynamic moment derivatives, which, in general, are much more important than the corresponding dynamic force derivatives. The two main categories of the dynamic moment derivatives (Table 1) are those due to pure rotation (p,q,r) and those due to the time rate of change of the two aerodynamic angles $(\dot{\alpha}, \dot{\beta})$. The latter is equivalent, in the first approximation, to the translational acceleration in the same plane of motion. In oscillatory experiments around a fixed axis, these two effects are present at the same time and, therefore, the results of such experiments are obtained as the sum of a pertinent rotary derivative and a pertinent acceleration derivative. Such sums are called *composite* derivatives. Depending on the degrees of freedom involved, we can further distinguish between the *damping* derivatives and the *cross* and *cross-coupling* derivatives, as indicated in the table.

Nonlinearities with Angle of Attack

Large variations with the angle of attack of the various complex flow features discussed in the previous section frequently cause significant nonlinearities in the dynamic stability parameters. Some examples of these nonlinearities are presented in Fig. 2, which shows two damping derivatives and one dynamic cross derivative obtained at NAE for a wing-body configuration at a Mach number of 0.7 (Ref. 5). These results amply illustrate both the magnitude and the suddenness of the variations in dynamic derivatives with the angle of attack. It can be appreciated that, if the angle of attack about which the oscillation takes place happens to be in the region where a sudden change in a derivative occurs, large effects of the amplitude of oscillation may be expected. In cases like this the derivative concept can only give an equivalent linearized description of the dependence of the aerodynamic reaction on the variable of motion and a better mathematical formulation may be needed.

Significant nonlinear effects were also obtained at NASA Langley[6,7] for fighter aircraft at low subsonic speeds. The damping-in-yaw derivative (Fig. 3) exhibits a very sudden and very large (ten times the low-α value and the sign reversed) unstable peak at angles of attack about 60 deg, while the two dynamic cross derivatives (Fig. 4) exhibit an equally large and sudden variation with α, but occurring at different values of that variable. It is interesting to note from these references that the angle of attack at which these peaks occur is largely independent of both the wing sweep angle and the presence of vertical tails, suggesting that the primary mechanism for these effects is associated with some flow phenomena located upstream of the wing and tails, a likely candidate being forebody vortices.

An example of the variation of a derivative with both the angle of attack and the oscillation amplitude is shown in Fig. 5, where the damping-in-roll derivative of a fighter configuration, obtained at NASA Langley[6] at low subsonic speeds, is plotted vs angle of attack. The large unstable peak that occurs at $\alpha = 35$ deg when the amplitude of oscillation is ± 5 deg decreases at larger amplitudes and completely disappears at an amplitude of ± 20 deg.

Nonlinearities with Rate of Roll (Spin)

Considerable nonlinearities with spin rate, together with important effects of both angle of attack and Reynolds

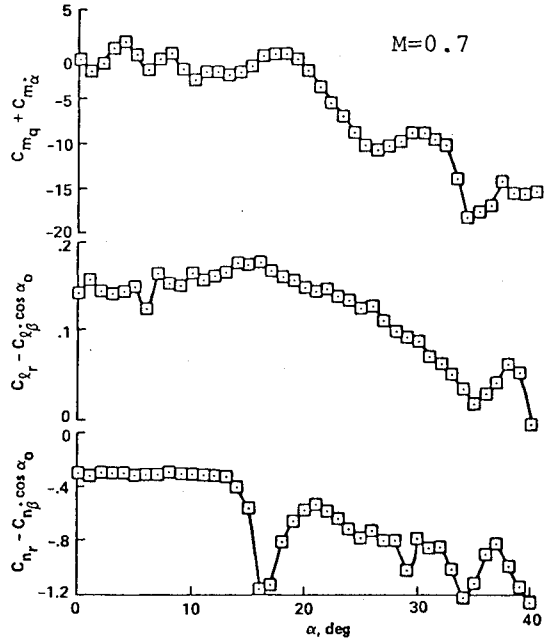

Fig. 2 Nonlinearities in damping and cross derivatives, $\Delta\theta = \Delta\psi = \pm 1$ deg (NAE).

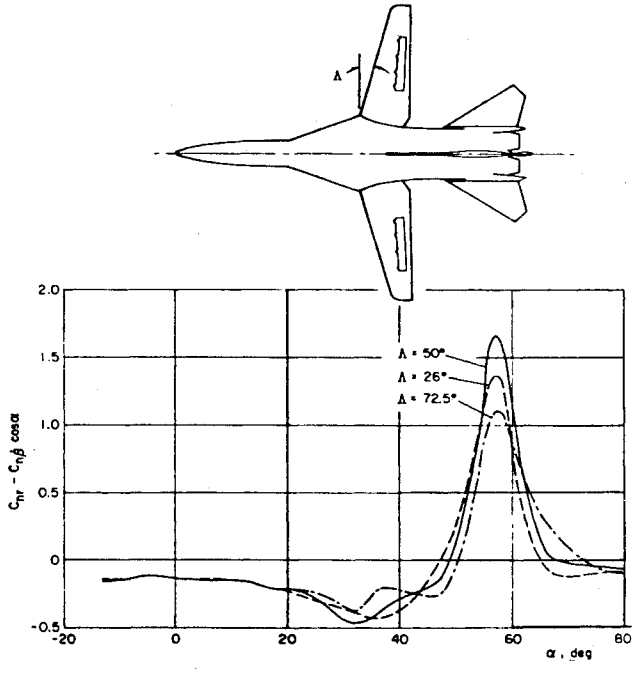

Fig. 3 Damping in yaw for a fighter configuration, $M < 0.1$, $\Delta\psi = \pm 5$ deg (NASA LRC).

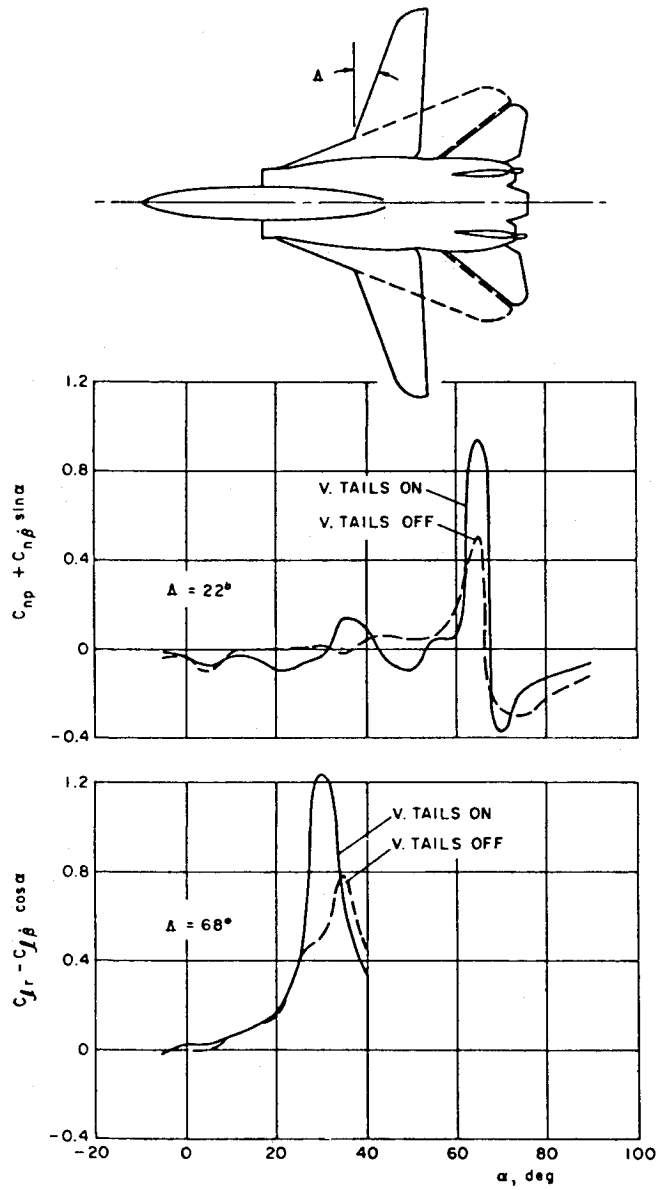

Fig. 4 Cross derivatives for a fighter configuration, $M<0.1$, $\Delta\phi = \Delta\psi = \pm 5$ deg (NASA LRC).

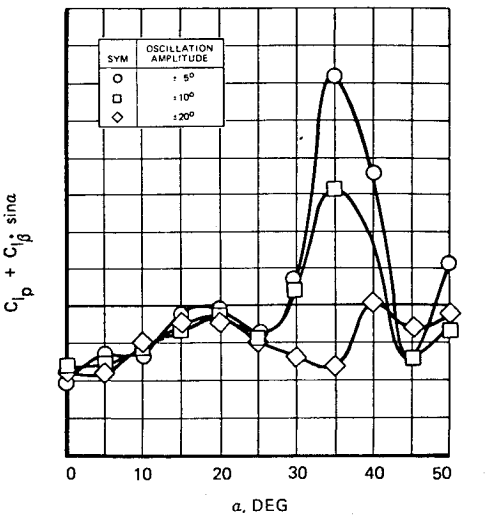

Fig. 5 Effect of oscillation amplitude on damping in roll (NASA LRC).

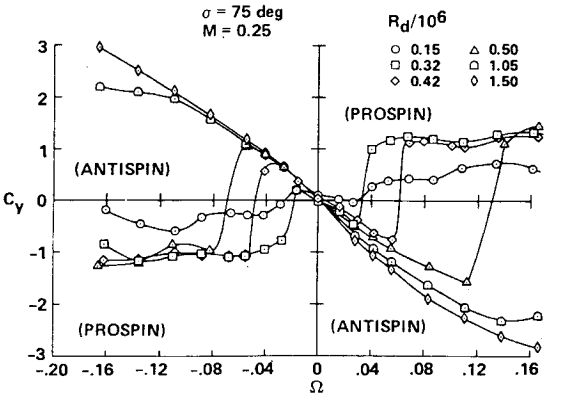

Fig. 6 Nose side-force coefficient vs reduced spin rate. Square cross section with rounded corners (NASA ARC).

number, are shown in Fig. 6, where the nose side-force coefficient for a model with a square forebody cross section but with rounded corners is shown as a function of the spin rate at $\alpha = 75$ deg and for various Reynolds numbers. These experiments, performed at NASA Ames Research Center,[8] show a strong nonlinear prospin contribution at all but the two lowest Reynolds numbers investigated. No such prospin contributions were detected at $\alpha = 45$ deg.

Another example[9] of large nonlinearities with spin rate is shown in Fig. 7. Pitching, rolling, and yawing moments for a series of general aviation models at $\alpha = 60$ deg are shown vs reduced spin parameter. The nonlinearity is pronounced and the sense of the rolling and yawing moments can change with rotation rate from autorotative to damping. The pitching moment increases most significantly over the static value, primarily due to the effect of the horizontal tail.

Occurrence of Wing Rock

An important manifestation of the effect of nonlinearities is the well-known phenomenon of wing rock. This phenomenon, primarily associated with the loss of damping in roll at higher angles of attack (Fig. 8), requires the presence of one or more nonlinear terms in the equation(s) of motion to render possible the characteristic limit-cycle type of oscillation in roll. It can be assumed that the aerodynamics of the problem, in principle, is related to the motion (or burst) of the forebody vortices or the leading-edge vortices, or else to the periodic variations from the attached to separated flow on some portion of the wing as the wing oscillates in roll. At transonic speeds an additional aerodynamic cause can be the periodic motion of the local shock waves. It is not yet well understood how these aerodynamic causes can be expressed mathematically in the equations of motion, but certain nonlinear terms have been experimentally determined and their effect on the resulting limit-cycle motion confirmed. Of course, different nonlinearities can be expected to exist for different configurations and different flight conditions. Three such scenarios, all involving wing rock at subsonic speeds, will be briefly described below.

Variation of Damping in Roll with Angle of Sideslip

The variation of the rolling moment with the reduced roll rate for various angles of attack and sideslip was recently studied at NASA Langley.[10] The data were obtained for an 80-deg delta wing at low subsonic speeds using a rotary balance (with the rotation taking place about the wind axis). Some of the results are shown in the upper part of Fig. 9. The slope of the curves represents the damping in roll and is negative for positive (stable) damping and vice versa. At $\alpha = 10$ deg the damping is positive for all β investigated. At $\alpha = 30$ deg the damping is negative at small β but positive at higher β. A set of curves (bottom left of Fig. 9) constructed by combining the above results with the results of some forced-oscillation experiments shows the variation of the damping in

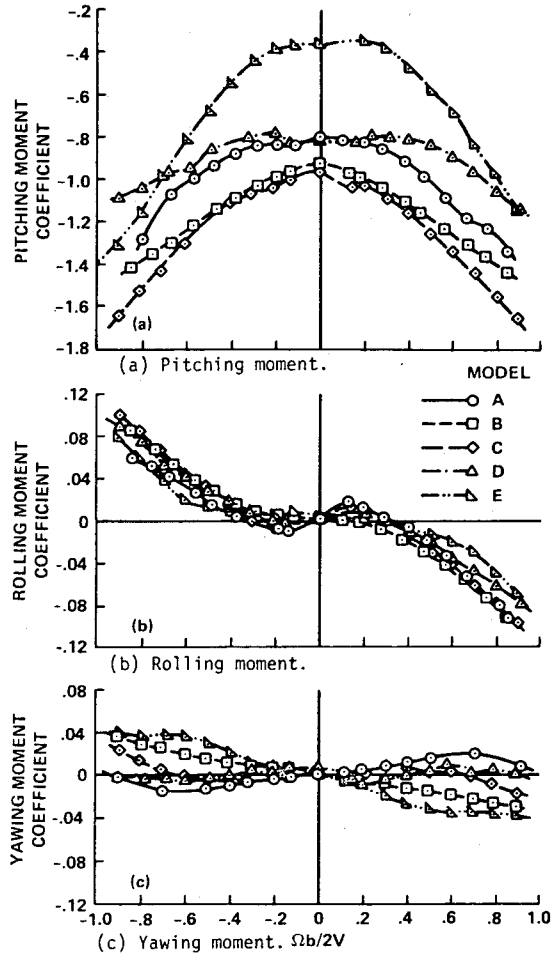

Fig. 7 Moment coefficients vs reduced spin rate. General aviation configuration, $\alpha = 60$ deg (NASA LRC).

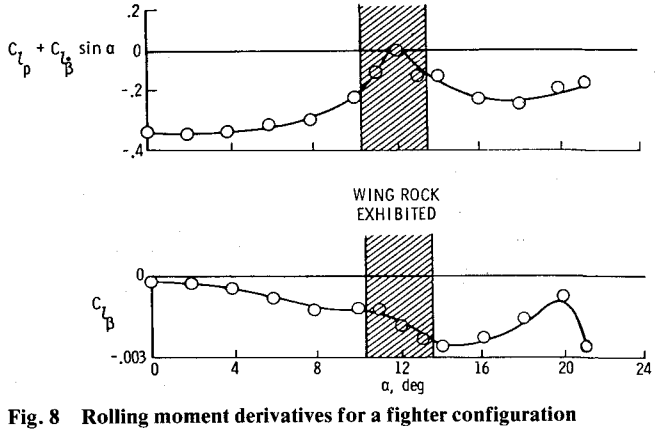

Fig. 8 Rolling moment derivatives for a fighter configuration (NASA LRC).

roll with the magnitude of sideslip for different angles of attack. The damping in roll changes from unstable to stable in the range of 5 to 7 deg of sideslip. Concurrent flow visualization studies (not shown) have indicated that this effect is associated with the upward displacement of the leeward vortex from the surface of the upgoing part of the wing, while the windward vortex remains close to the upper surface of the wing. A nonlinear simulation using these data yielded a wing-rock motion in close agreement with the results of a free-to-roll experiment, as can be seen on the bottom right of Fig. 9, where the comparison is shown in terms of the limit-cycle amplitude, $(\Delta\phi)_{WR}$, and the period, P_{WR}, of the wing rock observed at various angles of attack. Also shown are the results of an approximate analytical solution based on a simplified linear variation of the damping in roll with the magnitude of sideslip.

Cubic Variation of Lateral Derivatives with Roll Rate and Sideslip

The representation of the observed nonlinearities by the addition of a cubic term to certain static and dynamic stability derivatives was investigated at RAE.[11] It was shown that by including such a cubic term in the damping-in-roll derivative a fairly good agreement could be obtained between the flight and computed time responses for the roll rate and the angle of sideslip of a Gnat aircraft in a wing-rock situation (Fig. 10, top). It was also indicated that an inclusion of a similar cubic term in the cross derivative of the yawing moment due to the roll rate could probably have a beneficial effect on the prediction accuracy. In a separate study, cubic terms were introduced in the static yawing and rolling moment derivatives due to sideslip and it was shown that, although limit cycles could not normally be expected to occur through nonlinearities of a single-valued stiffness term in a second-order differential equation, such a limit cycle could and indeed did occur in a multimode system where the two stiffness terms were affecting both the frequency and the distribution of damping between the two modes involved (yawing and rolling). For a usual combination of the linear terms of the two derivatives ($l_{vI} > 0$, $n_{vI} > 0$) it was found (Fig. 10, bottom) that with a positive (stiffening) n_{v3} the limit cycle was predicted to occur for a large range of values of l_{v3}, while with a negative (softening) n_{v3} the limit cycle was computed only for $l_{v3} > 190$. Two different prediction methods (analog and approximate) were used in this study with good agreement. Since this type of nonlinearity in the moment derivatives due to sideslip can lead to divergence as well as to limit cycle, it was recommended that it be considered in the design of augmentation systems.

Aerodynamic Hysteresis in Steady-State Rolling Moment

Several reports[12-14] indicate the existence of aerodynamic hysteresis in the variation of the rolling moment coefficient with the angle of sideslip (or angle of roll) at higher angles of attack. Such hysteresis can be accounted for mathematically[15] by introducing into the aerodynamic formulation for the rolling moment a function $h(t)$ that can have two possible values in a given range of the angle of roll (Fig. 11, center). As shown in Ref. 15, for a fixed amplitude of oscillation the effective damping in roll can be expected to vary *inversely* with reduced frequency if the aerodynamic hysteresis is present, rather than *quadratically* as is normally the case without hysteresis. It was further shown in Ref. 15 that some early damping-in-roll results from NASA Langley[16] obtained for a twin-jet fighter aircraft at low subsonic speeds (Fig. 11, left) can be accurately correlated (with the exception of one point) by the expression for the effective damping in roll that takes into account the presence of hysteresis (Fig. 11, right). A formulation is suggested in Ref. 15 for the rolling moment in an arbitrary rolling maneuver (Fig. 11, bottom), which contains the double-valued function $h(t)$ and in which the effective damping-in-roll coefficient must be determined from roll oscillation around a fixed roll angle with the oscillation amplitude small enough to ensure that the deflection always remains on one branch of the hysteresis loop.

The aforementioned examples illustrate three possible scenarios for the occurrence of the wing rock, each on a different configuration. No doubt other such scenarios exist. When preparing the equations of motion for predicting the dynamic behavior of a new, unknown configuration, the mathematical model (at least initially) should be made sufficiently general to encompass all such scenarios.

Aerodynamic Cross-Coupling

The high-α flow phenomena discussed previously illustrate cases where 1) *lateral* aerodynamic reactions, such as those

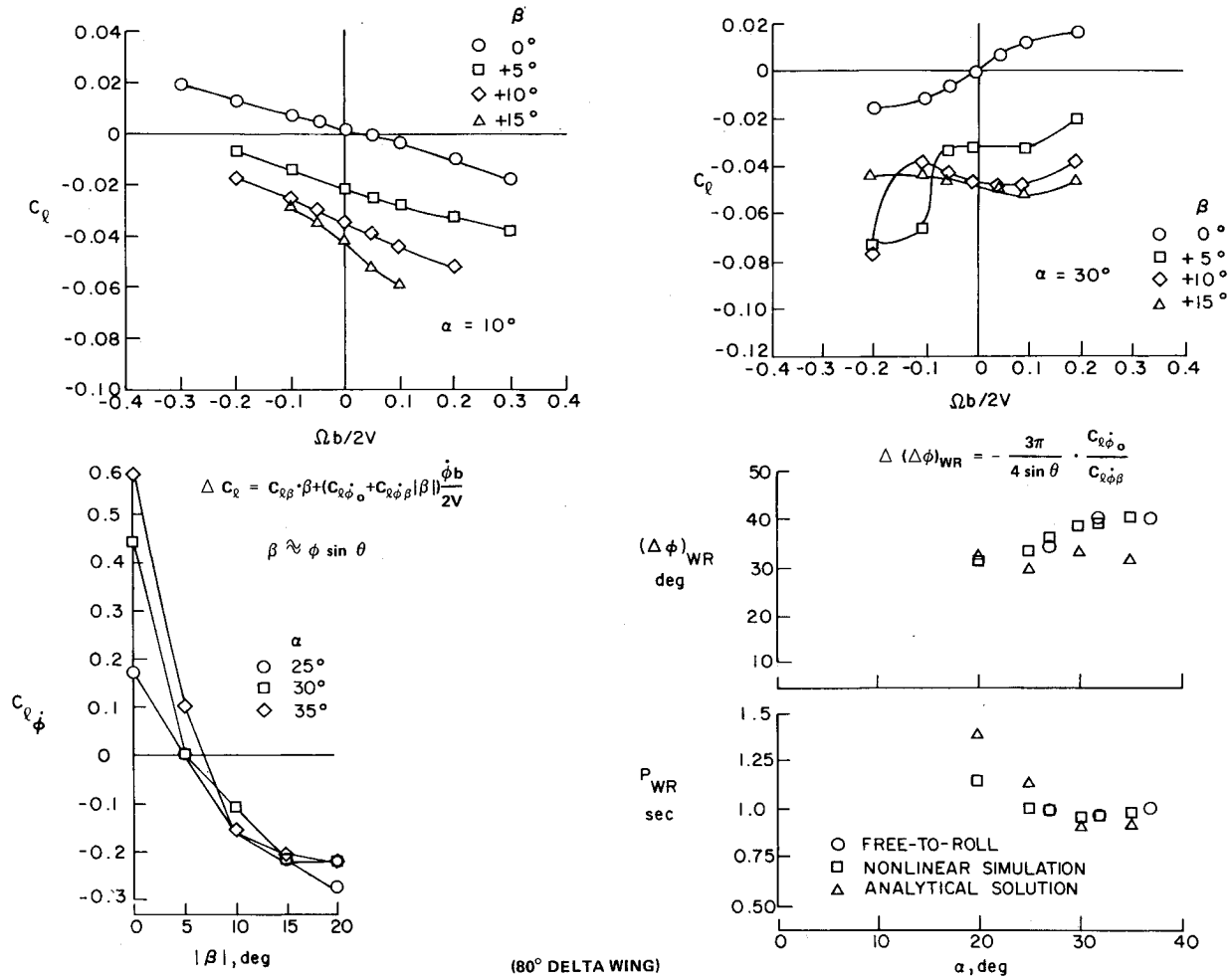

Fig. 9 Wing rock: variation of damping in roll with angle of sideslip (NASA LRC).

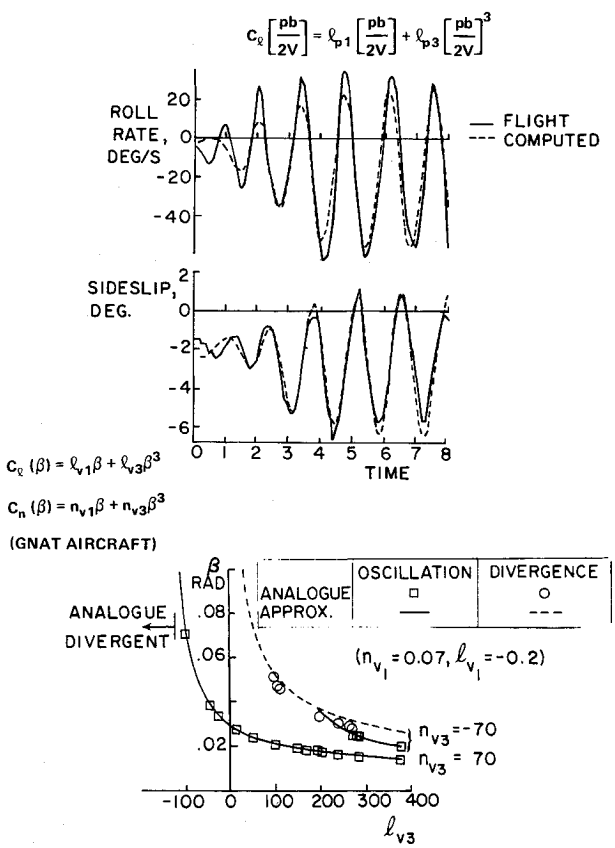

Fig. 10 Wing rock: cubic variation of lateral derivatives with roll rate and sideslip (RAE).

caused by the lateral motion of the forebody vortices, may occur on an aircraft as the result of some *longitudinal* motion, such as pitching or vertical translation, and where 2) *longitudinal* aerodynamic reactions, such as those caused by the longitudinal motion of the vortex burst locations, may occur on an aircraft as a result of some *lateral* motion, such as rolling, yawing, or lateral translation. Because of this relation between the longitudinal and lateral degrees of freedom, the above aerodynamic reactions can be said to represent the aerodynamic *cross-coupling* between the longitudinal and the lateral degrees of freedom. As already mentioned, the cross-coupling reactions are, in general, shifted in time in relation to their causative motions and, therefore, will have components which are both in phase and in quadrature with these motions. When related to the causative displacements and their time rates of change, these components of the cross-coupling reactions become static and dynamic *cross-coupling derivatives*, respectively. (The term *cross derivatives* should, however, still be used to denote the traditional derivatives that relate two lateral degrees of freedom, such as roll and yaw.) It should be noted that the introduction of cross-coupling derivatives requires simultaneous consideration of all the equations of motion of an aircraft, rather than of separate groups of equations for the longitudinal and for the lateral motions, as often done in the past.

The concept of aerodynamic cross-coupling, especially in relation to the dynamic derivatives, was introduced only relatively recently.[17] New experimental capabilities had to be developed to permit the measurement of the pertinent derivatives. Thus far, only relatively few measurements of this kind have been performed. Some examples of the dynamic cross-coupling derivatives obtained at NAE on a simple wing-body-fin configuration[5] are given in Fig. 12.

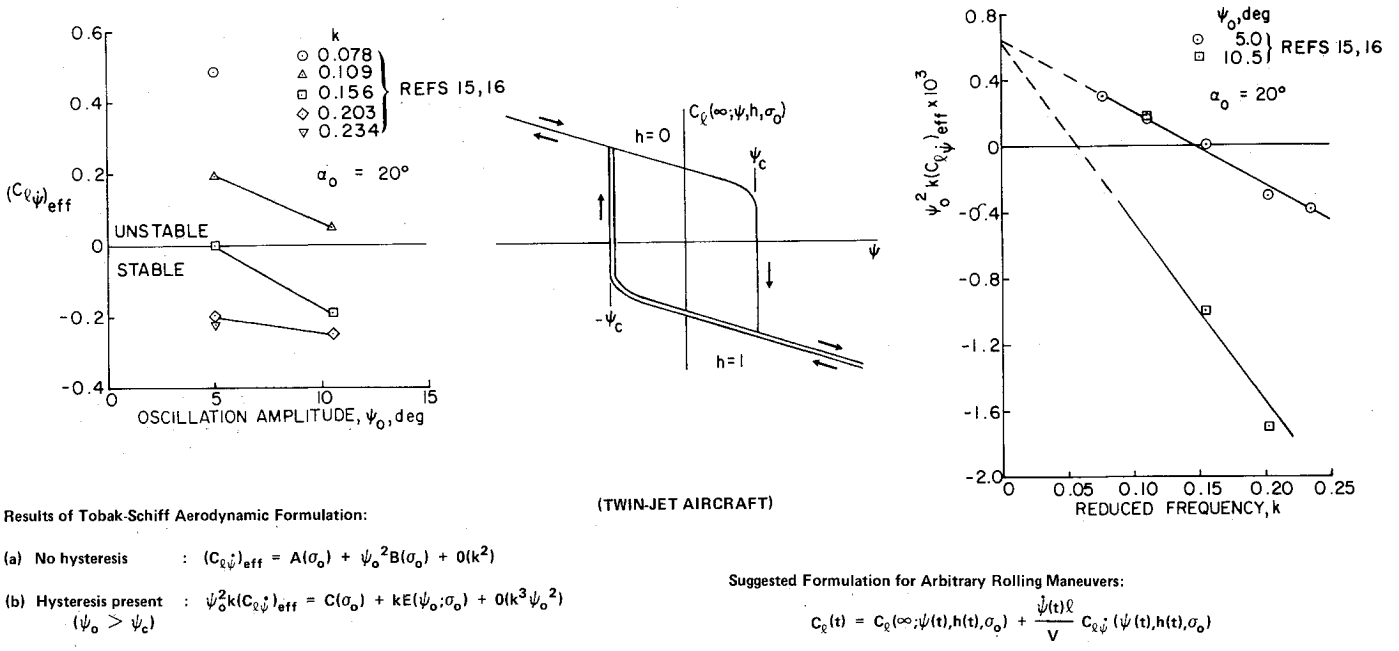

Fig. 11 Wing rock: aerodynamic hysteresis in steady-state rolling moment (NASA ARC; data measured at NASA LRC).

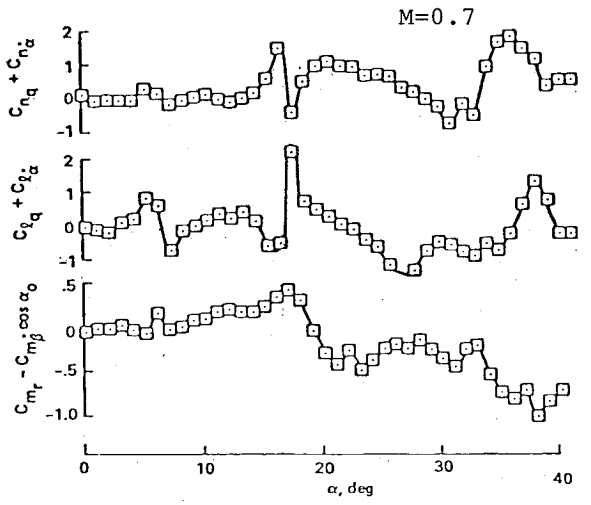

Fig. 12 Dynamic cross-coupling derivatives; wing-body-fin configuration; $\Delta\theta = \Delta\psi = \pm 1$ deg (NAE).

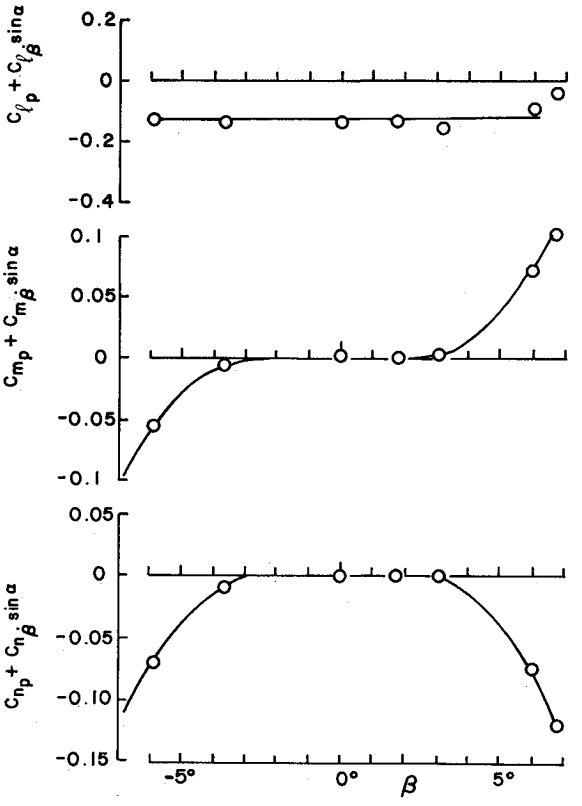

Fig. 13 Dynamic rolling moment derivatives vs angle of sideslip, $M = 0.6$; $\alpha = 17.5$ deg; $\Delta\phi = \pm 2$ deg (NAE).

From top to bottom, the dynamic yawing and rolling moment derivatives due to oscillation in pitch are shown, followed by the dynamic pitching moment derivative due to oscillation in yaw. In all cases, the derivatives are relatively small for low angles of attack, but attain large values and display sudden variations at angles of attack between 15 and 20 deg, and become quite irregular at higher angles of attack especially in the region between 32 and 38 deg. Both the levels attained and the suddenness of variations is larger for the derivatives of the lateral moments due to oscillation in pitch than for the pitching moment derivative due to oscillation in yaw. It should be noted that these cross-coupling derivatives may be of the same order, and sometimes even larger, than the corresponding traditional damping derivatives (except for the damping-in-pitch derivatives at high angles of attack), such as previously shown in Fig. 2. The same conclusion can also be reached when comparing, instead of the derivatives, the corresponding terms in the pertinent equations of motion.[5] Dynamic cross-coupling derivatives (at a Mach number of 0.6) were also measured at AEDC,[18] and the maximum values obtained were approximately one half of the maximum values obtained at NAE, which, considering the fact that the AEDC experiments were performed on a different configuration and in the angle-of-attack range of only up to 25 deg (rather than up to 40 deg at NAE), constitutes a good collaboration of the initial NAE results.

As can be expected from basic aerodynamic considerations, the direct and the cross derivatives should be symmetrical with respect to zero angle of sideslip, whereas the cross-coupling derivatives should change sign with the direction of sideslip. This is demonstrated in Fig. 13, where the three dynamic

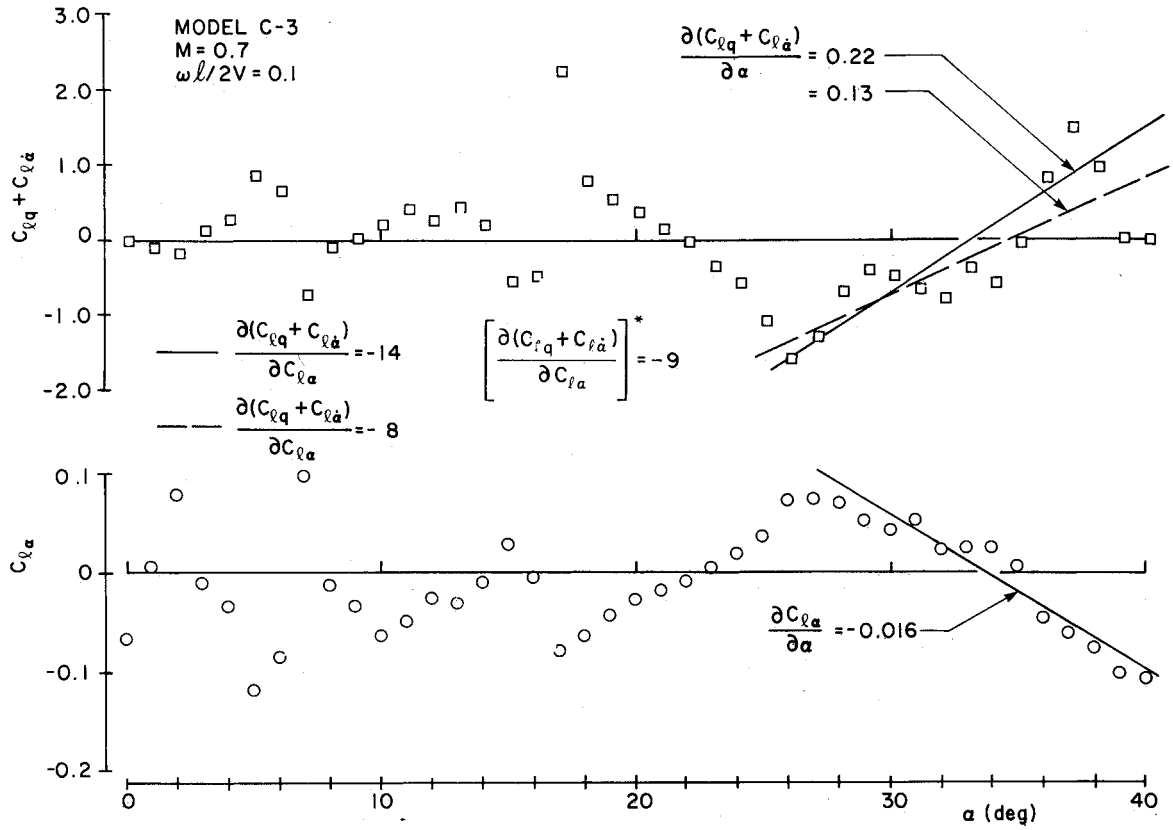

Fig. 14 Comparison of ratios of dynamic to static derivatives obtained in wind tunnel and calculated (*) using phase lag determined in water tunnel (NAE).

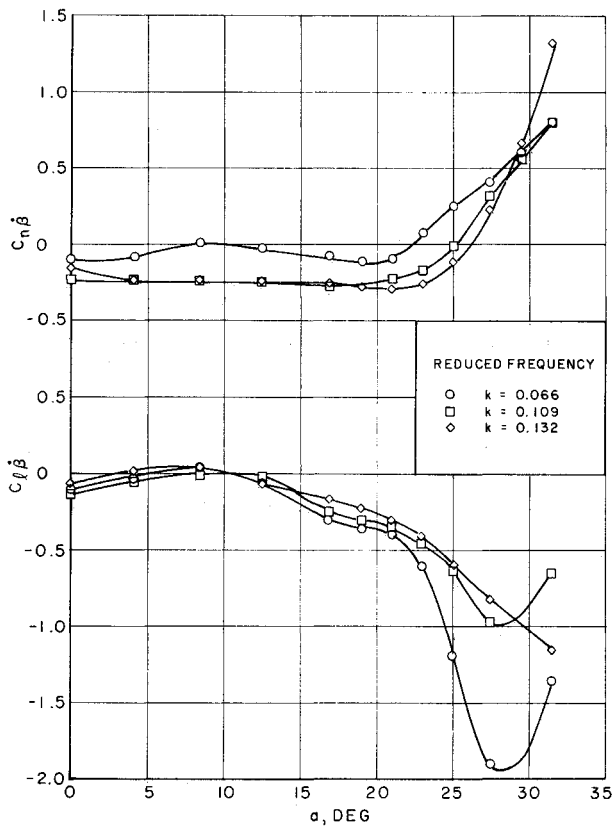

Fig. 15 $\dot{\beta}$-derivatives for a schematic delta-wing-body-tail configuration, $M < 0.1$ (NASA LRC).

moment derivatives due to oscillation in roll are plotted as functions of the angle of sideslip.[19] The antisymmetric variation of the cross-coupling derivative with the angle of sideslip is clearly visible. Another example of such a variation is given in Fig. 9 of Ref. 5.

For very simple configurations (such as the cone-wing-fin model used in the NAE movie), it may be possible to relate the dynamic derivatives to the corresponding static derivatives if the phase lag associated with the main flow-separation or vortex-shedding phenomenon is known. In Fig. 14 the ratio of dynamic-to-static rolling moment derivatives due to pitching obtained from such phase lag consideration (with the phase lag determined in the water tunnel, as shown in Fig. 1) is compared with the ratio of slopes of the two derivatives obtained on a similar (but not the same) configuration in a wind tunnel at a Mach number of 0.7. The ratios are of the same order of magnitude and the approximate mirrorlike symmetry of the dynamic and static curves is immediately apparent. The reader must be cautioned, however, that even if the phase lags could be easily measured or calculated (which, as a rule, they cannot), such a procedure would not necessarily be applicable to more realistic configurations, on which there would be a multitude of separated or vortical flow phenomena, each one with its own individual phase lag and each causing reactions acting on different parts of the configuration.

Time-Dependent Effects

In addition to quasisteady effects, such as represented by derivatives of various aerodynamic reactions due to angular velocities, we have to consider the existence of purely unsteady effects, such as those represented by derivatives due to the time rate of change of angular deflections, $\dot{\alpha}$ or $\dot{\beta}$. These derivatives have been known for many years, since they constitute part of the dynamic results obtained with standard wind-tunnel techniques of oscillation around a fixed axis,

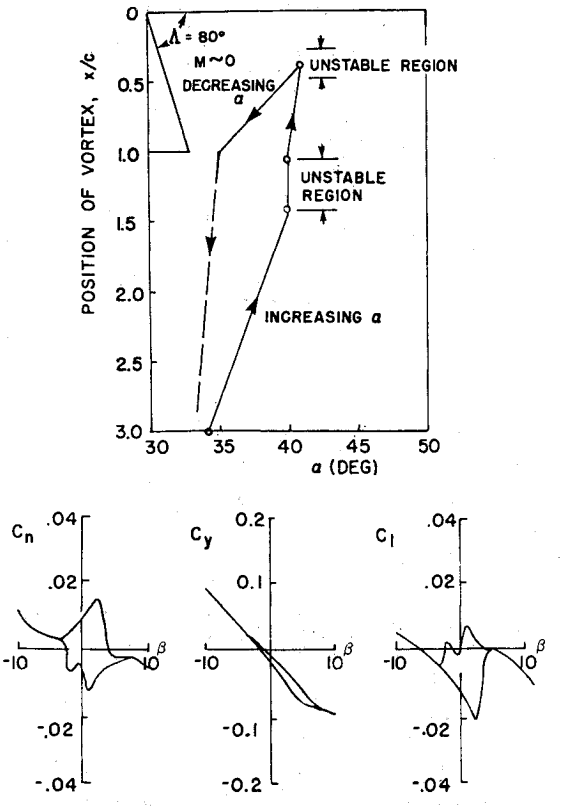

Fig. 16 Aerodynamic hysteresis a) with angle of attack, b) with sideslip.

which always give composite derivative expressions such as $(C_{mq}+C_{m\dot{\alpha}})$. Up to now, however, it was standard practice to ignore the $\dot{\alpha}$ and $\dot{\beta}$ effects (or to introduce a simple correction for them) and to use the composite derivatives in place of the purely rotary ones. At low angles of attack the error introduced by such a procedure was often small and the simplification large enough to be justifiable.

At higher angles of attack, however, the $\dot{\alpha}$ and $\dot{\beta}$ effects unfortunately become quite substantial and can no longer be ignored or corrected for in a simple fashion. This is illustrated in Fig. 15, based on Ref. 20, in which the yawing and rolling moment derivatives due to the time rate of change of the angle of sideslip are shown for a schematic delta-wing-body-tail configuration. These results were obtained from a translational oscillation experiment at very low speeds. The small values of the $C_{n\dot{\beta}}$ and $C_{l\dot{\beta}}$ derivatives at low angles of attack and their sudden increase at $\alpha \geq 22$ deg are clearly demonstrated.

Derivatives due to the time rate of change of angular deflections are aerodynamically equivalent (in the first approximation) to derivatives due to translational acceleration in the same plane of motion. This fact renders them of high interest for aircraft designs using direct-lift or direct side-force controls and also makes it possible to determine them experimentally using a translational oscillatory motion in the vertical or lateral direction. Because of this relation, $\dot{\alpha}$ and $\dot{\beta}$ derivatives are often referred to as translational acceleration derivatives.

Hysteresis Effects

As already discussed in connection with the wing-rock phenomenon, high angle-of-attack flow phenomena such as asymmetric vortex shedding, vortex breakdown (burst), or periodic separation and reattachment of the flow are frequently responsible for aerodynamic hysteresis effects. Such hysteresis is characterized by a double-valued behavior of the steady-state aerodynamic response to variations in one of the motion variables such as angle of attack, angle of sideslip, or spin rate. Figure 16 shows an α-hysteresis in the variation of location of the vortex burst on a delta wing,[21] and an example of the already described β-hysteresis in the variation of lateral aerodynamic coefficients for an aircraft configuration.[14] Figure 17 shows an example of an Ω-hysteresis in the side-force coefficient for the previously mentioned square forebody with rounded corners[8] rotating at $\alpha = 90$ deg (flat spin). (This hysteresis effect was not observed at $\alpha = 75$ deg and below, and even at $\alpha = 90$ deg it occurred only in a relatively narrow range of Reynolds number.) Another illustration of hysteresis effects is the delayed lateral motion of the forebody vortices in response to pitching oscillation, as shown in the aforementioned NAE water tunnel movie film.

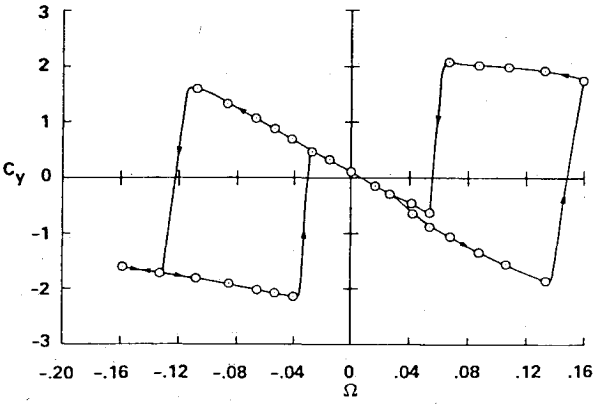

Fig. 17 Aerodynamic hysteresis with spin rate. Same experiment as in Fig. 6 but $\alpha = 90$ deg, $Re_d = 0.6 \cdot 10^6$ (NASA ARC).

In the presence of hysteresis the dynamic derivatives measured in large-amplitude oscillation experiments may have two distinct components, namely, one associated with the small-amplitude oscillation (i.e., small enough to remain on one branch of a hysteresis loop), and a second one representing the effect of the hysteresis. This was shown in Ref. 15 for the case of the damping-in-roll derivative. The large-amplitude oscillatory results, such as the magnitude of peaks shown in Fig. 4 (see Ref. 7), often display an inverse variation with frequency, which is characteristic of the presence of hysteresis. In such cases it must be remembered that the effective value of the derivative will depend on whether the oscillation amplitude falls inside or outside of the range that encompasses the hysteresis loop.

Configuration Dependence

The intricate vortex pattern that exists around an aircraft configuration at high angles of attack is very sensitive to even small changes in aircraft geometry. So is the behavior of this vortex pattern on an oscillating configuration. The forebody vortices are greatly dependent on the planform and the cross-sectional geometry of the aircraft nose as well as on the presence of various forms of protuberances on the forebody (including nose boom) that may affect the stability of an existing vortex pattern, give rise to new vortices and create conditions for strong vortex interactions. The wing leading-edge vortices, in addition to being a strong function of the leading-edge sweep, are also known to be greatly affected by various leading-edge modifications, such as apex drooping, discontinuities or contouring, and by various modifications of the wing itself, such as addition of wing leeside fences and deflections of leading- or trailing-edge flaps. All of these variations of the geometry of the wing affect not only the position and the strength of the wing vortices but also the all-important location at which these vortices break down.

The most common modification of the aircraft geometry intended to eliminate or delay the onset of asymmetric effects is the use of forebody strakes. Although, when used alone,

these strakes often prevent the formation of a unique vortex pattern at nonzero sideslip, thereby seriously reducing the directional stability of the configuration, they can be amazingly effective when used in combination with a suitable nose geometry. Figure 18 presents the effect of combining a leading-edge extension (LEX), which can be considered a form of strake, with a flat, broad nose (called the "Shark Nose") developed by Northrop,[14] on the variation with angle of attack of the dynamic directional stability parameter, $C_{n\beta DYN}$. The Shark Nose geometry, together with LEX, attenuates the unfavorable local reduction in that parameter and at the same time extends this favorable influence on stability to somewhat lower angles of attack. It has also been demonstrated in Ref. 14, (but is not shown here), that the presence of Shark Nose greatly enhances the directional stability at small nonzero angles of sideslip ($|\beta| < 5$ deg).

The effect of strakes (or leading-edge extensions) on various dynamic stability derivatives is illustrated in Fig. 19. In all cases shown, the addition of strakes reduces the magnitude of derivatives, practically eliminates nonlinearities with angle of attack in the range investigated (except for pitch damping derivative), and makes the derivatives almost independent of reduced frequency.[22] The dynamic yawing derivatives due to rolling become essentially zero. The

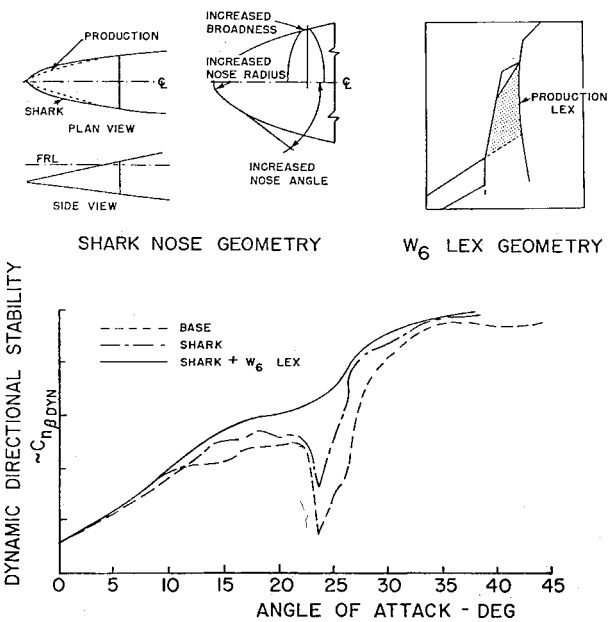

Fig. 18 Effect of forebody geometry and leading-edge extensions (Northrop).

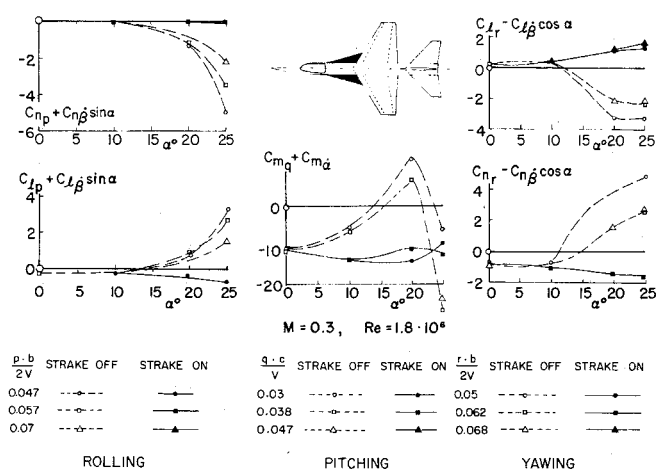

Fig. 19 Effect of strakes (MBB/ONERA).

Note 1:
With all aerodynamic cross coupling derivatives equal to zero, the rates p, r, and $\dot{\beta}$ remain essentially constant when perturbed in α; similarly the rates q and $\dot{\alpha}$ remain essentially constant when perturbed in β.

Note 2:
Angular rates for the unperturbed case remain constant and are denoted by p_0, q_0, r_0.

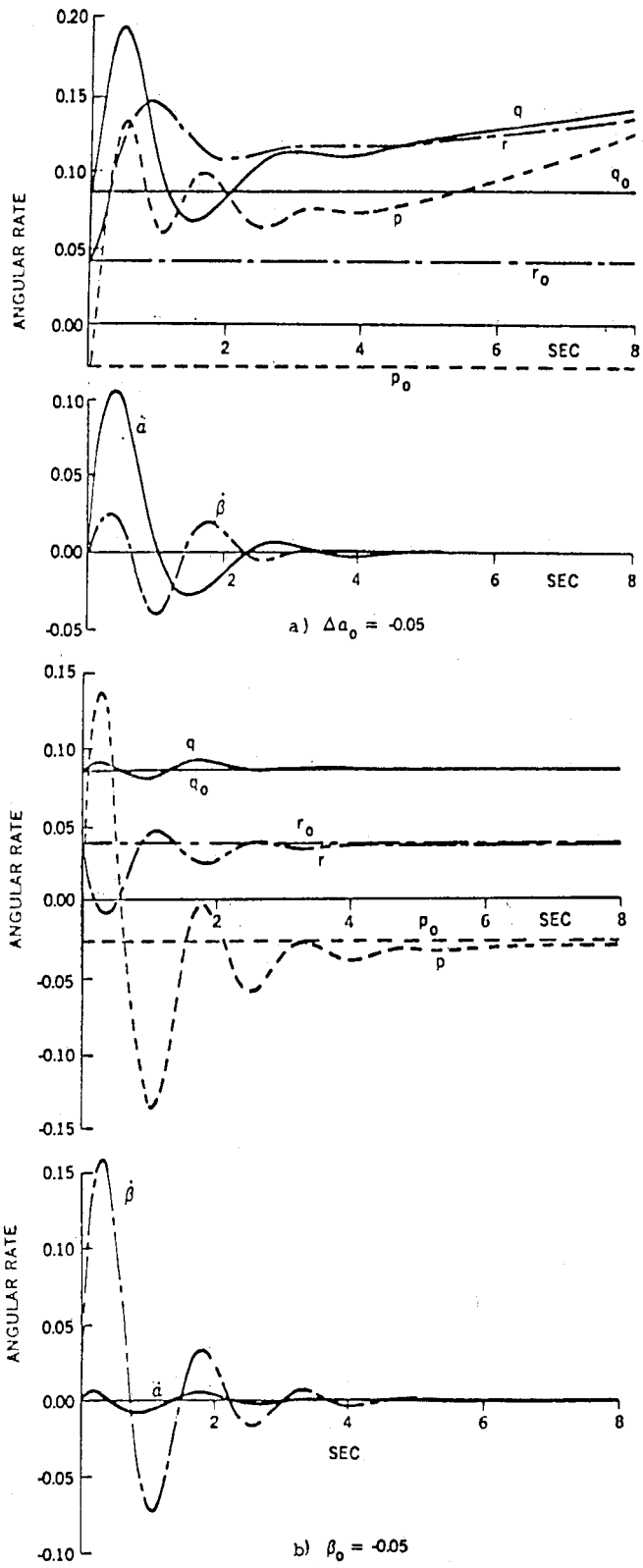

Fig. 20 Effect of cross-coupling derivates due to pitching and yawing on the angular rates for 2g turning flight (NAE).

negative damping in roll (for $\alpha > 13$ deg), in pitch (for $12 < \alpha < 23$ deg), and in yaw (for $\alpha > 11$ deg) completely disappears. It should be noted, however, that the range of angle of attack investigated extends only to $\alpha = 25$ deg, without reaching the range where the most significant nonlinearities may be expected.

As is well known, however, strakes do have certain disadvantages. Their successful development for a particular application may require much trial and error. They often adversely affect the directional stability. If mounted near the tip of the nose radome, they may disturb the radar operations. The strake vortices may adversely interact with aircraft components farther downstream, such as air intakes or control surfaces. Therefore, alternative approaches, such as the use of forebody blowing, forebody deflection, or a mechanical disturbance on the forebody, continue to be of high interest.

Although most of the important flow phenomena occur on the leeside of an aircraft, configuration changes on the windward side may also have a noticeable effect on the stability characteristics of the aircraft. For instance, an unsymmetrical store release can be expected to create aerodynamic cross-coupling effects, without even the necessity of flying at high angles of attack. The possible importance of such asymmetries is not very well known at the present time.

Sensitivity of High-α Aircraft Motion to Dynamic Stability Parameters

The need to introduce the dynamic cross-coupling and acceleration derivatives into the mathematical model, applicable to flight at high angles of attack, increases, in principle, the number of dynamic derivatives that may have to be included by a factor of two. This total number, however, can be significantly reduced if a judicious selection and assessment of the importance of some of these derivatives can be made. This is usually done by carrying out, on a computer, so-called "sensitivity studies," during which the sensitivity of the predicted aircraft behavior to the inclusion in the equations of motion of the cross-coupling and acceleration derivatives and of the taking into account the various nonlinear effects is examined. Some studies of this type have been performed in recent years and these were reviewed in Ref. 23, from which some examples will be included here.

Sensitivity studies are usually carried out by 1) programming, on a computer, a complete set of equations of motion pertinent to a particular configuration and particular flight condition, 2) inserting a set of stability parameters, including, if required, some nonlinear effects, 3) varying those parameters in a predetermined manner, and 4) observing the responses of the variables of motion to some form of disturbance applied to the set of equations. The stability parameters are usually varied individually, but may also be studied in combinations. The difference between responses obtained for two different values of a parameter or for two different combinations determines the sensitivity of the aircraft behavior to the variation of that particular stability parameter or that particular combination of parameters.

As already discussed, both the cross-coupling and the acceleration derivatives, and, in fact, most of the other derivatives as well, display significant nonlinear effects at higher angles of attack. Since an analytical description of the variation of a derivative with angle of attack may be rather complex, it is often more practical to limit the range of angle of attack, for which the analytical description is made, to the immediate vicinity of the equilibrium angle of attack and to assume that the derivative varies linearly with α in that narrow range of angle of attack. Such a locally linearized derivative can then be written as $a + b(\alpha - \alpha_T)$, when α_T is the trim (or equilibrium) angle of attack.

Dynamic derivatives that are subject to sensitivity study are often varied in a relatively wide range, such as from zero to perhaps twice the nominal value including, in some cases, also a change of sign. It is important that during such a variation the remaining derivatives be kept at their nominal values rather than zero, otherwise gross misrepresentation and, in some cases, even an erroneous elimination of the effect of a given derivative may result. Sometimes there may be some

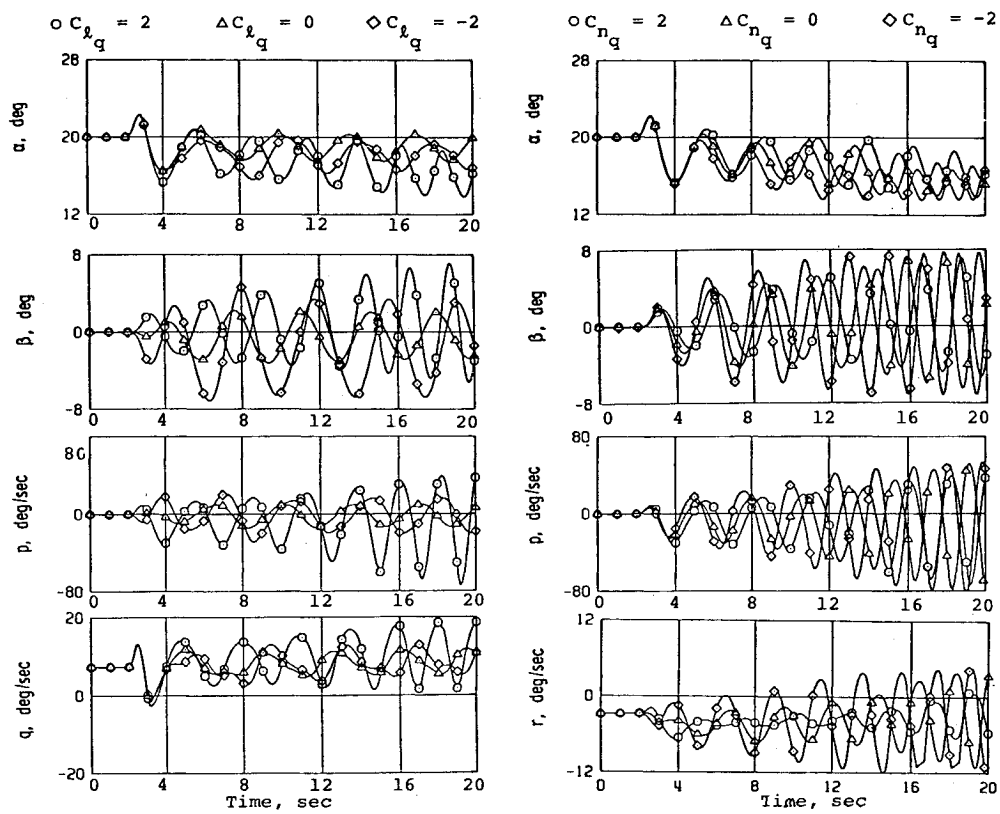

Fig. 21 Effect of C_{lq} and C_{nq} derivatives, fighter/bomber in 3g turning flight, $\dot{\beta}$ derivatives zero, elevator doublet (AEDC).

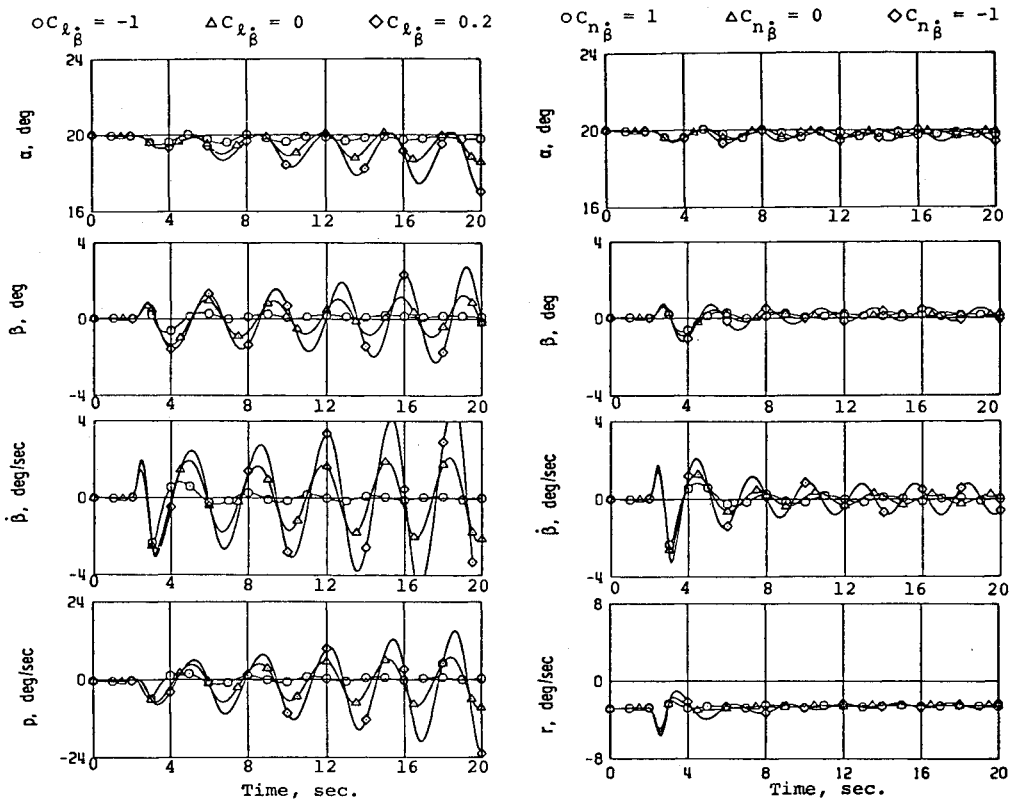

Fig. 22 Effect of $C_{l\dot\beta}$ and $C_{n\dot\beta}$ derivatives, fighter/bomber in 3g turning flight, rudder doublet (AEDC).

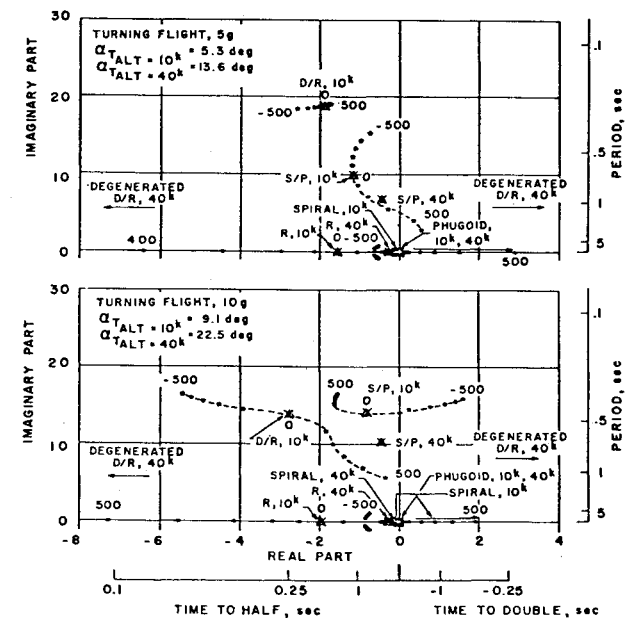

Fig. 23 Effect of C_{lq} derivative, yaw-to-turn missile in 10g turning flight, root locus (AEDC).

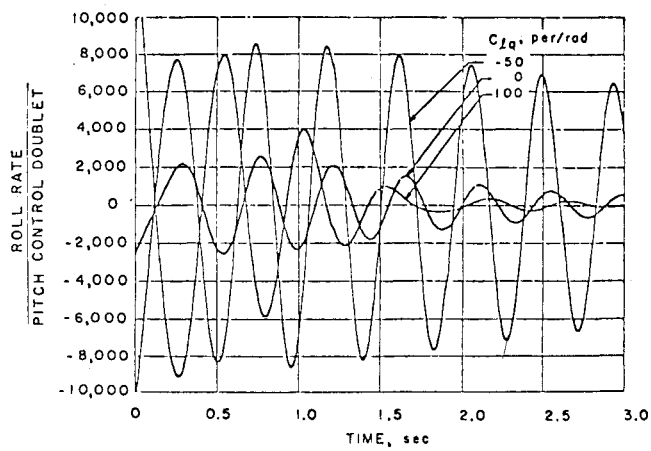

Fig. 24 Effect of C_{lq} derivative, yaw-to-turn missile in 10g turning flight, roll rate time history (AEDC).

interest in investigating the effect of a whole group of derivatives such as cross-coupling derivatives, by including or excluding the entire group all at once. In cases involving composite derivatives it is often of interest to divide the total value between the two component parts in different proportions and to insert the resulting two derivatives at their proper place in the equations of motion, as purely rotary and purely time-rate-of-change or acceleration effects.

The significance of cross-coupling moment derivatives was studied in Ref. 24 and is illustrated in Fig. 20. The measured values of composite derivatives were equally distributed between their rotary and acceleration parts. The nonlinear effects were taken into account by local linearization. The cross-coupling derivatives due to oscillation in roll were unknown at the time of the analysis and, therefore, set equal to zero. The various angular rates ($p,q,r,\dot\alpha$, and $\dot\beta$) are shown as functions of time after an initial disturbance in the angle of attack (Fig. 20a) and the angle of sideslip (Fig. 20b). The constant angular rates for the unperturbed case (p_0,q_0,r_0) are also shown. Had the cross-coupling derivatives not been included, the rates p, r, and $\dot\beta$ in Fig. 20a and the rates q and $\dot\alpha$ in Fig. 20b would have remained essentially constant. It can be seen that the departures of p, r, and $\dot\beta$ in Fig. 20a from their constant values is much larger than the corresponding departures of q and $\dot\alpha$ in Fig. 20b, indicating a much larger effect of the cross-coupling derivatives of the rolling and yawing moments due to pitching than of the cross-coupling derivative of the pitching moment due to yawing. Figure 20 pertains to a 2g turning flight at $\alpha = 33$ deg.

Studies of the sensitivity of the aircraft behavior to variation of an individual cross-coupling or acceleration derivative were carried out both in Refs. 24 and 25. Although

the two studies were performed using two significantly different approaches, the results were quite similar. Some examples of the results obtained in Ref. 25 for a fighter/bomber configuration in a 3g turning flight are shown in Figs. 21 and 22. In the study, the variations in each successive derivative were performed with all the other derivatives fixed at their nominal values. The cross-coupling derivatives were again based on the results of Ref. 5, but were treated as purely rotary derivatives in the equations of motion. The acceleration derivatives were based on data in Ref. 26. The nominal values used represented extreme values that had actually been measured in the wind tunnel experiments. The initial disturbance was introduced as an elevator or a rudder doublet.

Large effects of variations of both C_{lq} and C_{nq} can be seen in β, p, and r motions (Fig. 21). These motions display almost a mirror image for the positive and negative values of the pertinent derivatives. The inclusion of C_{lq} derivatives causes instability in the β and p motions. However, it should be noted that this effect is strongly dependent on the values of the remaining dynamic rolling moment derivatives, such as C_{lp} and $C_{l\dot{\beta}}$, which, in this particular example, were very small or zero, respectively.

The motion sensitivity to variations of $C_{l\dot{\beta}}$ derivative (Fig. 22) is quite significant. In particular, it should be noted that for $C_{l\dot{\beta}}$ values of 0.2 and greater, the α, β, $\dot{\beta}$, and p motions show strong oscillatory divergence. Conversely, the negative value of -1 of $C_{l\dot{\beta}}$ derivative has a strong damping effect on all of these motions. By comparison, the motion sensitivity to variations in $C_{n\dot{\beta}}$ is less significant.

Additional results, not shown here, indicate that most of the above-mentioned effects are quite dependent on the remaining stability characteristics of the aircraft. The smaller the static margin and the lower the aerodynamic damping, such as represented by C_{lp}, $C_{l\dot{\beta}}$, C_{nr}, or $C_{n\dot{\beta}}$ derivatives, the more sensitive the aircraft motion to the variations in cross-coupling derivatives and vice versa. The sensitivity of the flight behavior during a turning maneuver is, in general, larger than in a straight flight.

Although this paper is mainly concerned with stability and motion of aircraft, a brief mention has to be included about the corresponding studies related to the motion of missiles. A comprehensive investigation of missile motion sensitivity to dynamic stability derivatives has recently been completed.[27] In that investigation the importance of dynamic stability derivatives for the simulation of motion of both bank-to-turn and yaw-to-turn missile configurations was examined, using a six-degree-of-freedom linearized stability program.

Among the most pronounced effects due to the variation of a dynamic cross-coupling derivative was that due to the variation of C_{lq} at high Mach number, high load factor, and relatively low altitude. Sample results showing the influence of that derivative on the simulated motion of the yaw-to-turn missile are shown in Figs. 23 and 24. It can be seen that the short period (S/P), dutch roll (D/R), and roll (R) modes are quite sensitive to the variation of C_{lq} over the range ± 500 (per radian) and that the dutch roll sensitivity increases with an increasing load factor (Fig. 23). Even a variation of C_{lq} within a much more narrow range (0 to -50) results in a large effect on the roll rate time history (four times higher roll rates at $C_{lq} = -50$ than at $C_{lq} = 0$), as shown in Fig. 24.

On the basis of sensitivity studies, such as those described above, and on the basis of some additional studies included in Ref. 23, it has been shown that the inclusion in the equations of motion of the cross-coupling derivative C_{lq} (and to a lesser extent C_{nq}) and of the acceleration derivatives $C_{l\dot{\beta}}$, $C_{m\dot{\alpha}}$, and possibly $C_{l\dot{\alpha}}$ may be important for the correct prediction of the behavior of aircraft and missiles at high angles of attack (Table 2). It was shown in these studies that the aforementioned derivatives in some cases could have an effect on the predicted motion that was as large as that of some of the well-known damping and cross derivatives. It was also shown that it is important to be able to separate the purely rotary and the acceleration derivatives and use them in their proper places in the equations. Furthermore, it was found that the cross-coupling derivative C_{mp} is relatively important for missiles but less so for aircraft, and that the cross-coupling derivative C_{mr} appears to be insignificant in both of these cases.

Since the above studies were limited in scope with regard to both geometry of configurations and type of maneuvers, some of the derivatives found insignificant in these studies may become important in other situations. For a new aircraft or missile that has to perform a variety of maneuvers, the recommended set should encompass all the derivatives found important, even if only once, in previously examined situations. In addition, for a satisfactory prediction of aircraft behavior in a spin, the aerodynamic coefficients and possibly also the static and dynamic derivatives may be required as functions of spin rate.

Mathematical Modeling

The mathematical modeling used in most countries at the present time to describe the aircraft flight history applies strictly to flight at small to moderate angles of attack, where nonlinearities are small, time-dependent effects insignificant and aerodynamic cross-coupling nonexistent. In view of the complexity of the aerodynamic phenomena reviewed here and their effects on the forces and moments that govern the behavior of flight vehicles at high angles of attack, a much more sophisticated modeling is obviously required.

Substantial progress has recently been made in this area. A generalized formulation which includes the nonlinear pitch-yaw-roll coupling and nonlinear coning rate is now available.[28] Time-history and hysteresis effects have recently also been included in that formulation.[15,29,30] Among things still to be done is an adequate modeling of the suddenness with which the aerodynamic reactions may vary with the angle of attack or sideslip. As already mentioned, in the presence of such sudden and large nonlinearities, the derivative concept and the principle of linear superposition may no longer be adequate and a better mathematical formulation may be needed. One theory that offers considerable promise for adequate representation of sudden variations, hysteresis effects, and limit-cycle motions is the bifurcation theory, such as discussed in Ref. 31. It appears that this theory can also represent spinning as a genuine property of the appropriate set of differential equations.

Any advanced mathematical model must, of course, be suitably verified. The verification should be conducted by determining a complete set of stability parameters for a particular configuration, by predicting a series of maneuvers, and by comparing them with the actual flight histories. One of the principal difficulties in conducting such a verification at the present time is the lack of complete static and dynamic aerodynamic data for the required test cases.

Table 2 Relative significance of dynamic moment derivatives at high α (preliminary assessment)

Type of derivative(s)	Derivative(s)	Significant: Aircraft	Significant: Missiles
Direct	C_{mq}, C_{nr}, C_{lp}	Yes	Yes
Cross	C_{np}, C_{lr}	Yes	Yes
Cross-coupling	C_{lq}, C_{nq}	Yes	Yes
Cross-coupling	C_{mp}	No	Yes
Cross-coupling	C_{mr}	No	No
Acceleration	$C_{m\dot{\alpha}}$, $C_{l\dot{\beta}}$, $C_{l\dot{\alpha}}$	Yes	?
Acceleration	$C_{n\dot{\beta}}$, $C_{m\dot{\beta}}$, $C_{n\dot{\alpha}}$	?	?

Splitting of composite derivatives into component parts and using the different parts in their proper place in the equations of motion is in many cases important.

Aerodynamic coefficients and derivatives as functions of coning rate may be required for spin prediction.

Table 3 Dynamic stability testing capabilities at National Aeronautical Establishment

Apparatus	Primary motion	Static derivatives	Dynamic derivatives
Pitch/yaw	Pitching oscillation	$C_{l\alpha}$, $C_{m\alpha}$, $C_{n\alpha}$	$C_{lq}+C_{l\dot{\alpha}}$ $C_{mq}+C_{m\dot{\alpha}}$ $C_{nq}+C_{n\dot{\alpha}}$
Pitch/yaw	Yawing oscillation	$C_{l\beta}$, $C_{m\beta}$, $C_{n\beta}$	$C_{lr}-C_{l\dot{\beta}}\cos\alpha$ $C_{mr}-C_{m\dot{\beta}}\cos\alpha$ $C_{nr}-C_{n\dot{\beta}}\cos\alpha$
Roll	Rolling oscillation	$C_{l\beta}\sin\alpha$ $C_{m\beta}\sin\alpha$ $C_{n\beta}\sin\alpha$ $C_{Y\beta}\sin\alpha$ $C_{N_\beta}\sin\alpha$	$C_{lp}+C_{l\dot{\beta}}\sin\alpha$ $C_{mp}+C_{m\dot{\beta}}\sin\alpha$ $C_{np}+C_{n\dot{\beta}}\sin\alpha$ $C_{Y_p}+C_{Y\dot{\beta}}\sin\alpha$ $C_{N_p}+C_{N\dot{\beta}}\sin\alpha$
$\dot{\alpha}/\dot{\beta}$	Plunging oscillation	$C_{l\alpha}$, $C_{m\alpha}$, $C_{n\alpha}$	$C_{l\dot{\alpha}}$, $C_{m\dot{\alpha}}$, $C_{n\dot{\alpha}}$
$\dot{\alpha}/\dot{\beta}$	Lateral oscillation	$C_{l\beta}$, $C_{m\beta}$, $C_{n\beta}$	$C_{l\dot{\beta}}$, $C_{m\dot{\beta}}$, $C_{n\dot{\beta}}$
Pitch (half-model)	Pitching oscillation	$C_{m\alpha}$	$C_{mq}+C_{m\dot{\alpha}}$
Plunge (half-model)	Plunging oscillation	$C_{m\alpha}$	$C_{m\dot{\alpha}}$

New Dynamic Stability Test Techniques

The determination of a complete set of static and dynamic stability data for a test case of a high-angle-of-attack flight requires the availability of test techniques with the following, greatly expanded capabilities:

1) To test at high angles of attack, and to carry the associated high loads
2) To test at small to moderate angles of sideslip
3) To measure dynamic cross-coupling derivatives
4) To measure effects due to $\dot{\alpha}$ and $\dot{\beta}$
5) To measure effects due to coning and continuous rolling
6) To test at large amplitude of oscillation, particularly in the case of oscillation in roll.

A fairly complete review of existing testing techniques for determination of dynamic stability parameters in a wind tunnel was given by the present author in Ref. 32. This review included the significant developments that have taken place in the last few years at several research establishments in various countries of the world, and notably those at NASA Ames, NASA Langley, AEDC, RAE Bedford, BAC Warton, DFVLR, ONERA, and NAE. Since the development of experimental techniques plays such an important role in our progress toward obtaining better prediction capabilities of the aircraft behavior in high-angle-of-attack flight, this topic clearly deserves to be mentioned in the present paper. As an example, a brief account will be rendered of the techniques presently available at the NAE in Ottawa, which may be considered as fairly representative of the new experimental trends in this field.

In Table 3 a list is given of the presently available three full-model and two half-model apparatuses that can be used to study the primary oscillations in five degrees of freedom, providing means to determine all the moment derivatives and some of the force derivatives associated with these motions. Both static and dynamic derivatives are included and the list encompasses the direct, cross, and cross-coupling derivatives, as discussed previously. It should be noted that in all cases the derivatives are obtained from a direct measurement, which is based only on an assumed relation between the aerodynamic reaction measured and the causative primary motion. Often this relation is linear, but can be replaced by a nonlinear or higher-order formulation if the need arises. Since the motion

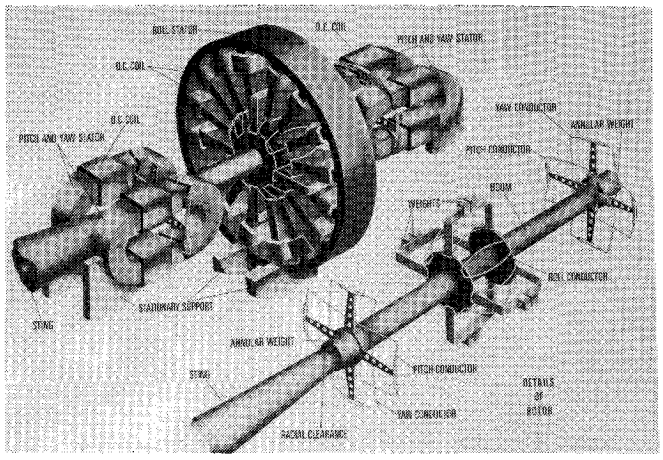

Fig. 25 3-DOF dynamic calibrator (NAE).

is essentially in one degree of freedom, the measurement is independent of the remaining parts of the equations of motion and, therefore, the results may be expected to be valid for any formulation of these equations as long as the principle of superposition is still applicable.

In most of the full-model apparatuses the model is mounted on a balance that in turn is attached to an elastic support system capable of deflecting in the appropriate degree of freedom. The primary motion is imparted by an electromagnetic drive system which oscillates the model with a constant amplitude at the resonance frequency in the primary degree of freedom. Each balance has a multicomponent capability (but always without axial force) and is made in one piece, a most desirable feature for dynamic testing. Each drive mechanism utilizes a high-current coil (or coils) moving in a strong magnetic field that is generated by compact rare-earth permanent magnets. As a result, the apparatuses are relatively slender and permit testing of realistic models of current aircraft configurations. Other apparatuses, employing a mechanical drive system, are used for experiments performed in the presence of large aerodynamic restoring moments. More details about the NAE apparatuses and test techniques can be found in Refs. 32 and 33.

The high complexity of the aforementioned techniques and the lack of any previous data on some of the recently identified dynamic derivatives made it necessary to develop a system that would independently verify the validity of the experimental technique and data reduction methods employed. The same system was also conceived as a diagnostic tool to identify, on a regular basis, equipment faults or software errors. A pictorial view of such a system developed at NAE and called a dynamic calibrator is shown in Fig. 25. The aircraft model is replaced on the dynamic stability apparatus by a special calibrating frame (or "rotor"), which is then oscillated in the primary degree of freedom by the drive mechanism of the apparatus. The inertia characteristics of the rotor duplicate, at least approximately, the inertia characteristics of the model, resulting in a similar dynamic response of the rotor and of the model in all three degrees of freedom. The three oscillatory aerodynamic moments, that act on the oscillating model during a wind tunnel test, are simulated by accurately known, electromagnetically induced, alternating loads, whose phase and amplitude can be adjusted at will. A comparison between the known applied loads and the outputs of the dynamic stability apparatus, obtained by processing the balance data and other relevant information by means of the same procedure as in the wind tunnel experiments, provides an overall calibration of the technique and of all the mechanical and electronic systems involved. Other dynamic calibrators, simpler but based on similar principles, have been developed for the half-model dynamic apparatuses.

When conducting dynamic experiments in a wind tunnel, careful attention must be given at all times to minimizing and/or correcting for the inevitable static and dynamic sting interference effects. These problems were extensively discussed in Refs. 34 and 35. Also of great concern is the possible seriousness of Reynolds number effects. At high angles of attack the aerodynamic characteristics are often dominated by separated flow effects and it is known[36] that the boundary-layer transition process may also depend on the vehicle motion. Hence the possibilities for simulating flight Reynolds numbers by means of boundary-layer tripping devices in subscale dynamic experiments (as often proven successful in static experiments) are more limited. No universally accepted simulation methods seem to exist at the present time. Very few, if any, reliable comparisons of dynamic derivatives obtained at high angles of attack in flight and in wind tunnel are available, and those that do exist may easily be affected not only by the difference in the Reynolds numbers, but also by support interference problems in wind tunnel testing on the one hand and the need for a preconceived mathematical model and a practical (not too large) number of the unknown parameters (to be solved for) in flight testing on the other. It is, therefore, rather difficult to draw any definite conclusions as to the seriousness of the problem. There are some indications, however, that in many cases the dynamic behavior of the aircraft, as observed in flight tests, drop model tests and spin tunnel experiments, shows a fair overall agreement, despite the large differences in test Reynolds numbers.[14,37] Any such observations are likely to be strongly dependent on the configuration being tested.

Concluding Remarks

In this paper a review was presented of some of the aerodynamic phenomena associated with the dynamic behavior of an aircraft flying at high angles of attack and of the various effects that these phenomena have on the dynamic stability parameters of aircraft or missiles at those flight conditions. Although only very limited quantitative information on these effects is available at the present time, an attempt was made to offer a tentative assessment of the relative significance of the various effects and parameters. The deficiencies of the commonly used mathematical models of the aerodynamics of high-angle-of-attack maneuvers were pointed out and the need was postulated for the development and verification of more sophisticated models that would probably have to include significant nonlinearities, hysteresis, some aerodynamic cross-coupling, and some time-dependent effects. Finally, developments in the wind tunnel techniques needed to provide the aerodynamic inputs required for such more advanced mathematical modeling were discussed and illustrated by examples of some of the novel techniques that have been developed at the author's laboratory.

References

[1] "High Angle of Attack Aerodynamics," AGARD FDP Symposium, Sandefjord, Norway, Oct. 1978, AGARD-CP-247, 1979.

[2] Tobak, M. and Peake, D.J., "Topology of Three-Dimensional Separated Flows," *Annual Review of Fluid Mechanics,* Vol. 14, 1982, pp. 61-85.

[3] Skow, A.M., Moore, W.A., and Lorincz, D.J., "Control of Forebody Vortex Orientation to Enhance Departure Recovery of Fighter Aircraft," *Journal of Aircraft,* Vol. 19, Oct. 1982, pp. 812-819.

[4] Peake, D.J. and Owen, F.K., "Control of Forebody Three-Dimensional Flow Separations," Paper 15, AGARD-CP-262, 1979.

[5] Orlik-Rückemann, K.J., "Aerodynamic Coupling Between Lateral and Longitudinal Degrees of Freedom," *AIAA Journal,* Vol. 15, Dec. 1977, pp. 1792-1799.

[6] Chambers, J.R., Gilbert, W.P., and Nguyen, L.T., "Results of Piloted Simulator Studies of Fighter Aircraft at High Angles of Attack," Paper 33, AGARD-CP-235, 1978.

[7] Grafton, S.B. and Anglin, E.L., "Dynamic Stability Derivatives at Angles of Attack from $-5°$ to 90° for a Variable-Sweep Fighter Configuration with Twin Vertical Tails," NASA TN D-6909, 1972.

[8] Malcolm, G.N., "New Rotation-Balance Apparatuses for Measuring Airplane Spin Aerodynamics in the Wind Tunnel," *Journal of Aircraft,* Vol. 16, April 1979, pp. 264-268.

[9] Birhle, W. Jr. and Bowman, J.S. Jr., "Influence of Wing, Fuselage and Tail Design on Rotational Flow Aerodynamics Beyond Maximum Lift," *Journal of Aircraft,* Vol. 18, Nov. 1981, pp. 920-925.

[10] Nguyen, L.T., Yip, L., and Chambers, J.R., "Self-Induced Wing Rock of Slender Delta Wings," AIAA Paper 81-1883, Aug. 1981.

[11] Ross, A.J., "Lateral Stability at High Angles of Attack, Particularly Wing Rock," Paper 10, AGARD-CP-260, 1978.

[12] Ottensoser, J., "High Angle of Attack Aerodynamic Data for a 0.10 Scale A-7 Model Evaluated in the 7 by 10-Foot Transonic Wind Tunnel for Investigating the Stall Departure Phenomena, Phase 1," NSRDC TM-16-76-16, Oct. 1975.

[13] Herman, J.G. and Washington, E.S., "Wind Tunnel Investigation of the Aerodynamic Hysteresis Phenomenon on the F-4 Aircraft and its Effects on Aircraft Motion," AEDC-80-10, Sept. 1980.

[14] Skow, A.M. and Titiriga, A. Jr., "A Survey of Analytical and Experimental Techniques to Predict Aircraft Dynamic Characteristics at High Angles of Attack," Paper 19, AGARD-CP-235, 1978.

[15] Schiff, L.B. and Tobak, M., "Some Applications of Aerodynamic Formulations to Problems in Aircraft Dynamics," Lecture 16, AGARD-LS-114, 1981.

[16] Grafton, S.B. and Libbey, C.E., "Dynamic Stability Derivatives of a Twin-Jet Fighter Model at Angles of Attack from $-10°$ to 110°," NASA TN D-6091, Jan. 1971.

[17] Orlik-Rückemann, K.J., "Dynamic Stability Testing of Aircraft—Needs Versus Capabilities," *Proceedings of International Congress on Instrumentation in Aerospace Simulation Facilities,* 1973, pp. 8-23.

[18] Coulter, S.M. and Marquart, E.J., "Cross and Cross-Coupling Derivative Measurements on the Standard Dynamics Model at AEDC," AIAA Paper 82-0596, 1982.

[19] Hanff, E.S., Orlik-Rückemann, K.J., Kapoor, K.B., Moulton, B.E., and LaBerge, J.G., "New Oscillatory Roll Apparatus and Results on Direct, Cross and Cross-Coupling Subsonic Moment Derivatives for an Aircraft-Like Model," NRC, NAE LTR-UA-50, 1979.

[20] Lichtenstein, J.H. and Williams, J.L., "Effect of Frequency of Sideslipping Motion on the Lateral Stability Derivatives of a Typical Delta-Wing Airplane," NACA RM L57F07, 1957.

[21] Lawson, M.V., "Some Experiments with Vortex Breakdown," *Journal of the Royal Aeronautical Society,* Vol. 68, May 1964, pp. 343-346.

[22] Staudacher, W., Laschka, B., Schulze, B., Poisson-Quinton, P., and Canu, M., "Some Factors Affecting the Dynamic Stability Derivatives of a Fighter-Type Model," Paper 11, AGARD-CP-235, 1978.

[23] Orlik-Rückemann, K.J., "Sensitivity of Aircraft Motion to Cross-Coupling and Acceleration Derivatives," Lecture 15, AGARD-LS-114, 1981.

[24] Curry, W.H. and Orlik-Rückemann, K.J., "Sensitivity of Aircraft Motion to Aerodynamic Cross-Coupling at High Angles of Attack," Paper 34, AGARD-CP-235, 1978.

[25] Langham, T.F., "Aircraft Motion Sensitivity to Dynamic Stability Derivatives," AEDC-TR-79-11, 1980.

[26] Coe, P.L. Jr., Graham, B.H., and Chambers, J.R., "Summary of Information on Low-Speed Lateral-Direction Derivatives Due to Rate of Change of Sideslip, $\dot{\beta}$," NASA TN D-7972, 1975.

[27] Langham, T.F., "Missile Motion Sensitivity to Dynamic Stability Derivatives," AIAA Paper 81-0400, 1981.

[28] Tobak, M. and Schiff, L.B., "On the Formulation of the Aerodynamic Characteristics in Aircraft Dynamics," NASA TR R-456, 1976.

[29] Tobak, M. and Schiff, L.B., "The Role of Time-History Effects in the Formulation of the Aerodynamics of Aircraft Dynamics," Paper 26, AGARD-CP-235, 1978.

[30] Tobak, M. and Schiff, L.B., "Aerodynamic Mathematical Modelling—Basic Concepts," Lecture 1, AGARD-LS-114, 1981.

[31] Guicheteau, P., "Application de la théorie des bifurcations à l'étude des pertes de contrôle sur avion de combat," Paper 17, AGARD-CP-319, 1981.

[32] Orlik-Rückemann, K.J., "Review of Techniques for Determination of Dynamic Stability Derivatives in Wind Tunnels," Lecture 3, AGARD-LS-114, 1981.

[33]Hanff, E.S., "Direct Forced-Oscillation Techniques for the Determination of Stability Derivatives in Wind Tunnels," Lecture 4, AGARD-LS-114, 1981.
[34]Ericsson, L.E., "Support Interference," Lecture 8, AGARD-LS-114, 1981.
[35]Beyers, M.E., "Measurement of Direct Moment Derivatives in the Presence of Sting Plunging," NAE-AN-1, 1983.
[36]Ericsson, L.E. and Reding, J.P., "Scaling Problems in Dynamic Tests of Aircraft-Like Configurations," Paper 25, AGARD-CP-227, Sept. 1977.
[37]Chambers, J.R., DiCarlo, D.J., and Johnson, J.L. Jr., "Applications of Dynamic Stability Parameters to Problems in Aircraft Dynamics," Paper 17, AGARD-LS-114, 1981.

Bibliography

[1]"Unsteady Aerodynamics," AGARD FDP Symposium, Ottawa, Canada, AGARD-CP-227, Sept. 1977.
[2]"Dynamic Stability Parameters," AGARD FDP Symposium, Athens, Greesce, AGARD-CP-235, May 1978.
[3]"High Angle of Attack Aerodynamics," AGARD FDP Symposium, Sandefjord, Norway, AGARD-CP-247, Oct. 1978.
[4]"Dynamic Stability Parameters," AGARD FDP Lecture Series, NASA ARC, USA and VKI, Belgium, AGARD-LS-114, March 1981.
[5]"High Angle of Attack Aerodynamics," AGARD FDP Lecture Series, NASA LRC, USA, VKI, Belgium, and DFVLR, Gottingen, Germany, AGARD-LS-121, March 1982.
[6]Tischler, M.B. and Barlow, J.B., "Dynamic Analysis of the Flat Spin Mode of a General Aviation Aircraft," *Journal of Aircraft*, Vol. 19, March 1982, pp. 198-205.
[7]Carroll, J.V. and Mehra, R.K., "Bifurcation Analysis of Nonlinear Aircraft Dynamics," *Journal of Guidance, Control and Dynamics*, Vol. 5, Sept.-Oct. 1982, pp. 529-536.
[8]Bihrle, W. Jr. and Barnhart, B., "Spin Prediction Techniques," *Journal of Aircraft*, Vol. 20, Feb. 1983, pp. 97-101.
[9]Hui, W.H. and Toback, M., "Bifurcation Analysis of Nonlinear Stability of Aircraft at High Angles of Attack," AIAA Paper 82-0244, 1982.